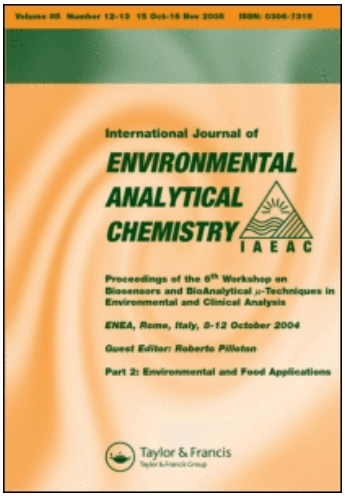

International Journal of Environmental Analytical Chemistry
Publication details, including instructions for authors and subscription information:
http://www.informaworld.com/smpp/title~content=t713640455

Mass Size Distributions and Precursor Gas Concentrations of Major Inorganic Ions in'Antarctic Aerosol

Risto Hillamo[a]; Ivo Allegrini[b]; Roberto Sparapani[b]; Veli-Matti Kerminen[a]
[a] Finnish Meteorological Institute, Helsinki, Finland [b] CNR/Institute for Atmospheric Pollution, Monterotondo Scalo (Roma), Italy

To cite this Article Hillamo, Risto , Allegrini, Ivo , Sparapani, Roberto and Kerminen, Veli-Matti(1998) 'Mass Size Distributions and Precursor Gas Concentrations of Major Inorganic Ions in'Antarctic Aerosol', International Journal of Environmental Analytical Chemistry, 71: 3, 353 — 372
To link to this Article: DOI: 10.1080/03067319808032638
URL: http://dx.doi.org/10.1080/03067319808032638

Intern. J. Environ. Anal. Chem., Vol. 71(3-4), pp. 353-372
Reprints available directly from the publisher
Photocopying permitted by license only

MASS SIZE DISTRIBUTIONS AND PRECURSOR GAS CONCENTRATIONS OF MAJOR INORGANIC IONS IN ANTARCTIC AEROSOL

RISTO HILLAMO[a], IVO ALLEGRINI[b*], ROBERTO SPARAPANI[b] and VELI-MATTI KERMINEN[a]

[a]*Finnish Meteorological Institute, Air Quality, Sahaajankatu 20 E, FIN-00810 Helsinki, Finland and* [b]*CNR/Institute for Atmospheric Pollution, Via Salaria 29,3 km, I-00016 Monterotondo Scalo (Roma), Italy*

(Received 18 July 1996; In final form 30 April 1997)

Mass size distributions of major inorganic ions in aerosol particles and their atmospheric precursor gases were studied at Terra Nova Bay in Antarctica (74° 41 ′42 ″S, 164° 05 ′36 ″E) between January 30 and February 18, 1995. The mass size distributions of sulphate, the major inorganic ion, had two submicron and two supermicron modes. The accumulation mode (average mass median diameter 0.285±0.016 μm) had a very stable concentration over the whole sampling period (238.8±39.7 ng/m^3). The smaller submicron mode (Aitken mode) had an averaged mass median diameter at 0.069 μm (standard deviation 0.011 μm). The existence of an Aitken mode is an indirect indication of new particle formation in the Antarctic summer atmosphere. The coarse-particle sulphate is due to the emissions of sea salt particles and their subsequent absorption of and reactions with atmospheric SO_2. Ammonium was found primarily in the accumulation mode, where it probably was associated with very acidic ammonium sulphate/hydrated sulphuric acid particles. Other detected ions were sodium, magnesium, chloride and nitrate, all of them found mainly in coarse-particle size range and related to sea-salt particles and their subsequent heterogenous reactions with gaseous compounds. Concentration ranges of HNO_2, HNO_3, SO_2 and NH_3 where 18.9–23.9, 20.9–39.1, 38.1–60. 1 and 31.2–52.7 ng/m^3. respectively.

Keywords: Antarctica; Polar atmosphere; inorganic ions; impactors; denuders

INTRODUCTION

Compared with polar Northern-hemisphere regions which are exposed to pollutants from industrialized areas in Eurasia and Europe for most of the time, high

* Corresponding author. Fax: +39–6–90672660. E-mail: allegrini@ntserver.iia.mlib.cnr.it

latitudes in the Southern hemisphere are relatively free from anthropogenic influence. The major continental, natural sources for the Antarctic air pollution are volcanos, and emissions from penguin populations [1, 2]. Seas are an important source of both primary and secondary compounds found in the Antarctic troposphere. Especially during the austral summer, the open oceans surrounding the Antarctic continent release large quantities of various inorganic and organic species to the atmosphere [3, 4].

It has now been widely recognized that understanding and predicting the global climate change requires incorporation of aerosol particles in climate models [5, 6]. Particles affect the Earth's radiation balance directly by scattering and absorbing incoming solar light, and indirectly via their effects on cloud properties. The sign of both direct and indirect aerosol forcing is expected to be negative (cooling). Inorganic ionic species play a central role in both cases. From the dry mass of accumulation-mode particles (mass median diameter at around 0.5 μm), which commonly account for more than 90% of the direct radiative forcing due to aerosol particles [7], typically some 40 to 60% comes from major inorganic ions. In addition to this, inorganics dictate to a large extent particle hygroscopic properties, which are of prime importance in assessing both direct and indirect aerosol radiative forcing.

Modelling climatic and other influences due to aerosol particles requires information on the spatial and temporal distribution of the particle number concentration and chemical composition as a function of the particle size. Knowing the sources for particles and their precursor gases is essential for understanding and quantifying the secondary processes that modify particle populations during their residence in the atmosphere. An example of a major particulate precursor whose atmospheric concentrations are influenced significantly by both natural and anthropogenic sources is sulphur dioxide. Anthropogenic SO_2 is mainly due to energy production by fossil fuel combustion and to nonferrous ore smelting, while natural SO_2 originates almost entirely from dimethyl sulphide (DMS) released to the atmosphere by phytoplankton blooming on ocean surfaces [8, 9]. Atmospheric DMS is oxidized rapidly to methane sulphonic acid (MSA) and sulphate, both of which are found predominantly in the particulate phase [10].

This paper summarizes results from a field experiment carried out at Terra Nova Bay (74° 41 ′42 ″S, 164° 05 ′36 ″E), Antarctica, between January 30 and February 18, 1995. The experiment involved measuring the concentrations and mass size distributions of inorganic ionic compounds with impactor size spectroscopy, as well as measuring the concentrations of particle precursor gases with annular denuders. The primary goal of this study was to examine tropospheric multi-phase chemistry in an environment affected dominantly by natural sources of air pollutants.

EXPERIMENTAL

Diffusion denuder/filter pack

Excluding a few modifications given below, the experimental set up of the electronically-controlled diffusion denuder sampler used in this study was similar to that described in Allegrini et al. [11]. For the present study there was no cyclone in the sampling line due to technical problems, but a denuder for ammonia collection was included. Instead of sodium chloride, the first two denuders were coated with sodium fluoride. A backup filter was used to collect ammonia and acidic gases released from the front filter. The denuder line was operated with a 24-hour sampling duration.

Low pressure impactor

Impactors have widely been used to collect size-segregated particle samples for chemical analysis. The impactor type used in this study was a copy of the commercial Berner low pressure impactor model 25/0.015 [12]. The impactor has ten stages covering the particle size range of 0.035–15 μm. The volume flow rate of air through the impactor is 25 L/min at sea level. The aerodynamic cut-off diameters (particle sizes corresponding to the 50% collection efficiency) of the impactor stages are shown in Table I. The impactor collects and classifies particles in the size range one expects to be important in remote polar areas for aerosol mass size distribution.

TABLE I Aerodynamic cutoff diameters of the low pressure impactor. Calculated at conditions 980 hPa and 278K

Stage number	*Aerodynamic cutoff diameter, μm*
Inlet	15.9
11	15.9
10	7.75
9	4.29
8	2.25
7	1.12
6	0.564
5	0.336
4	0.173
3	0.095
2	0.067
1	0.035

The sampling set up is shown schematically in Figure 1. The sample inlet was outside the cabin, whereas the impactor, the vacuum pump (Leybold SV 25), the vacuum line with a needle valve and a vacuum gauge, were inside. The inlet was connected using a 20-cm-long adapter with the impactor. Both the inlet and the impactor were oriented vertically. The purpose of the inlet was to prevent snow and water from penetrating the impactor, and to make the coarse-particle sampling efficiency independent of the wind speed [13]. Two identical impactors were used; when the first one was sampling, the other one was unloaded, cleaned and prepared for sampling.

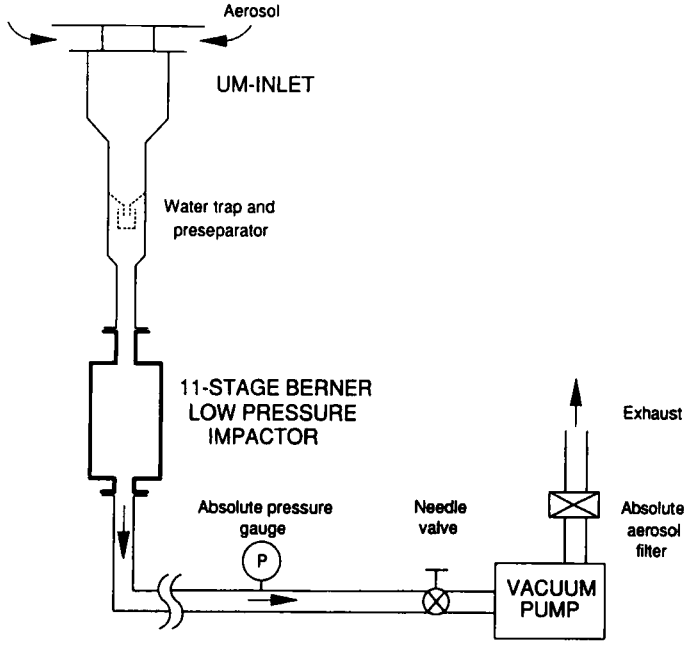

FIGURE 1 The experimental field set up for impactor sampling

The air flow through the nozzles of the lowest impactor stage was kept critical by regulating the pressure downstream of the impactor to a value of 85 mbar using a needle valve. This ensures a constant mass flow over the sampling period, because the impactor had no back up filter which might change the pressure drop. The air temperature of the flow downstream of the impactor was not measured, which causes some uncertainties in calculated sample volumes. While the outside temperature varied from 0 to −14 °C, the air-conditioned and heated cabin was permanently around +20 °C. Since the temperature response in the

impactor is not known, it is difficult to account for variations in the ambient temperature over the long sampling period (48 h). As a compromise. it was assumed that the sample air warms up little inside the impactor and a constant value of +5°C was used in calculating the sample volumes.

Polycarbonate films were used as impaction substrates (poreless film from Nuclepore Inc., thickness 10 μm). To prevent, or reduce, the particle bounce off when they hit the collection substrate, all films were coated with vacuum grease. Coatings were made using a toluene solution of the Apiezon L vacuum grease. The solution was painted onto the substrate with a brush. After evaporation of the toluene, a quite uniform grease layer covering the approximate sample deposit area under the impactor nozzles was obtained.

Chemical analysis of denuder and impactor samples

To avoid possible losses and artifacts during storage, most samples were analysed immediately after sampling. The substrates were first cut into pieces and placed in test tubes for extraction with 8–10 ml of deionized water. Analysis was conducted by ion chromatography (Dionex DX-100) using a 50 μl loop and the Dionex AS 12 column for anions and the Dionex CS 12 column for cations. Limits of detection and quantification are shown in Table II. Results of K^+ and Mg^{2+} in the impactor data were not used because of high blank values in the extraction solution. Runs 9 and 10 of the impactor samples were analysed in the chemical laboratory several weeks after the sampling. Both Cl^- and NH_4^+ are susceptible to distortion during storage, and were therefore discarded from the data sets of runs 9 and 10.

TABLE II Detection (DL) and quantification (QL) limits in ion chromatograph analysis (ng/ml)

	Cl^-	NO_2^-	NO_3^-	SO_4^{2-}	NH_4^+	Na^+	K^+	Mg^{2+}	Ca^{2+}
DL	3	5	10	15	5	1	5	2	5
QL	10	15	30	45	15	3	15	6	15

RESULTS AND DISCUSSION

Measurement site

The measurement site was located in a clean area on the top of a hill northwest of the Italian Antarctic research camp in Terra Nova Bay. The distance between the

sampling site and the main camp was 400 meters. The camp is a potential contamination source to the local atmosphere. The major activities causing pollutant releases are waste handling (storage and limited burning), and power generation by two 90 kW diesel generators. Although possible contamination due to the main camp was not monitored, it probably had no or minor influence on measured concentrations because the prevailing wind direction was usually in the clean sector. The wind data over the sampling period is shown in Figure 2. The dominating wind directions 210°-330° are in the clean sector, and cover 68 % of the measurement time.

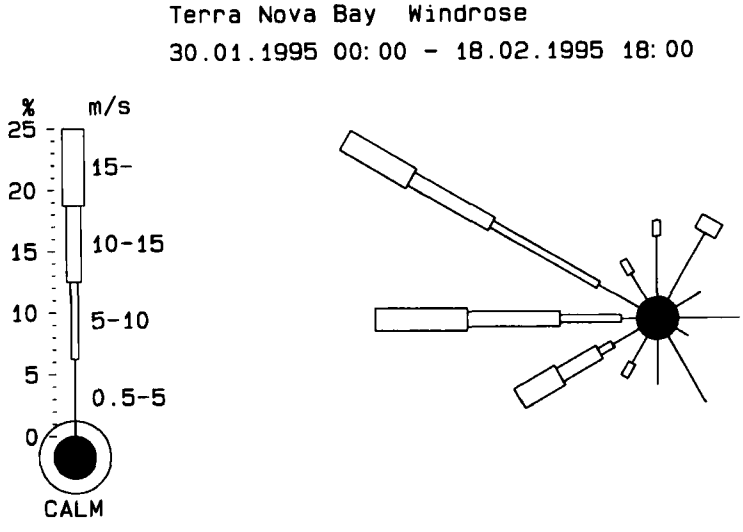

FIGURE 2 Wind statistics in Terra Nova Bay meteorological station over the field period of this study

Another potential contamination source during the sampling period was an oil supply ship (Feb. 5–6). During the filling of the camp's oil tanks, the ship was anchored north of the measurement site. Winds during this period were in the sector 270°-330°. However, no traces of contamination of ship diesel engine exhausts can be identified from the data.

Diffusion denuder/filter pack

The lack of a cyclone upstream of the denuder line may lead to contamination of the annular denuder tubes by coarse-particle deposition. Therefore, the gas con-

centrations presented here are limited to periods with low coarse-particle concentrations. The periods were chosen according to the data in Figure 5. The results, together with data from some other studies, are shown in Table III. The original 24-hour denuder data were averaged to correspond to 48-hour impactor runs. For the period February 15–16 only SO_2 concentration is shown, since those samples were analysed in the laboratory several weeks after the sampling, being subject to artifacts and to obvious losses of semi-volatile compounds during the storage.

TABLE III Concentrations of some gaseous components (ng/m^3) during selected impactor runs[1)]

Date	*Impactor Run*	*HNO_2*		*HNO_3*		*SO_2*		*NH_3*	
		Ave	*STD*	*Ave*	*STD*	*Ave*	*STD*	*Ave*	*STD*
Jan 30–31	1	22.5	7.7	22.6	7.5	55.9	10. 1	52.7	14.5
Feb 3–4	3	18.9	2.6	39.1	5.9	60.1	11.9	39.3	7.0
Feb 7–8	5	23.9	0.9	20.9	14.0	40.2	12.9	31.2	11.3
Feb 15–16	9	-	-	-	-	38.1	9.61	-	-
South Pole, ref. (1)		-	-	-	-	-	-	16.0	
Antarctic marine boundary layer, ref. (14)						45–450			

1) Samples of Feb 15–16 were analyzed in the laboratory after the field campaign and the data of HNO_2, $HNO_3$and NH_3 are discarded due to potential risk of losses or artifacts

According to Gras [14] concentrations of SO_2 may vary in the range 45–450 ng/m^3 in the Antarctic marine boundary layer. The highest values are from sub-Antarctic areas and may be influenced by long-range transported anthropogenic pollution. Thus, the SO_2 concentrations measured in the present study are consistent with levels observed in Antarctic clean polar areas in previous studies. The ammonia concentrations measured in the present study range from 31.2 to 52.7 ng/m^3, consistent with the mean ammonia concentration of 16 ng/m^3 measured in a cleaner environment, the Amundsen-Scott station, at the South-Pole [1].

Impactor data: inversion and mode fitting

A data set of an impactor run consists of a series of ionic concentrations (ten for each ion) found by chemical analysis of the substrates from the different impactor stages. Each stage has a certain cut-off diameter: in an ideal case the stage

collects all particles larger than this cut-off size, while particles smaller than that size penetrate the stage. The impactor stages are in series, thus the upper limit of a stage is set by the preceding stage. Although the impactor stages never have the "ideal" collection characteristics, traditionally the step function has been used to approximate the real S-shaped response function (collection efficiency vs. particle diameter). The result is a discrete size distribution given typically in a differential form $\Delta m/\Delta \log D_p$, where Δm is the mass concentration found in the stage and $\Delta \log D_p$ is the difference of logarithms of stage size boundaries. Using this simplified approach, the size resolution of an impactor usually is good enough to detect the modal nature of atmospheric aerosols with a geometric standard deviation typically varying between 1.3–2.0. A more accurate approach in the data reduction, the data inversion, can be employed if the impactor response (the S-shaped collection efficiency curve for each stage) is known.

The data inversion technique is advantageous for the evaluation of impactor data, enabling the use of the accurate collection efficiency curves instead of approximate step functions. The inverted size distributions are closer to real ones than those in the step-functional approach. The inverted size distributions can also give continuous information on the species' mass as a function of particle size. The raw data of this study were inverted using the MICRON data inversion code [15]. In the inversion, the calibrations of Wang and John [16] and Hillamo and Kauppinen [17] were used for the response of the Berner low pressure impactor. The inverted size distribution is based on a single solution, which is found using the stagewise concentration data and the corresponding experimental errors. As a simple quality check, the inverted distribution were always compared with the discrete size distribution and with the total concentration of the raw data. In a proper inversion they should agree. More detailed discussion on the potential problems related to impactor data inversion are discussed by Kerminen et al. [18].

Atmospheric aerosols usually have distinct particle size modes. Each mode is frequently related to a different formation mechanism, such as photochemical, cloud processing or mechanical disintegration. The modes can be presented by means of statistical functions, the most common of which is a log-normal distribution. In this work the mode fitting was conducted using a software developed by Winklmayer et al. [19] and modified further at the University of Gent.

Particle size distributions

The measured anion and cation mass size distributions are shown in Figures 3 and 4, respectively. Over the coarse-particle size range (particle aerodynamic diameter greater than 1 μm), ten complete data sets for sulphate. chloride,

sodium and magnesium, were obtained. The nitrate size distribution could be constructed from runs 1–5, 9 and 10. Technical difficulties in the water purification system caused quite high blank values for Ca and K, and insufficient number of data points to determine their size distributions were available. For the same reason nitrate data for runs 6–7 were considered uncertain and discarded.

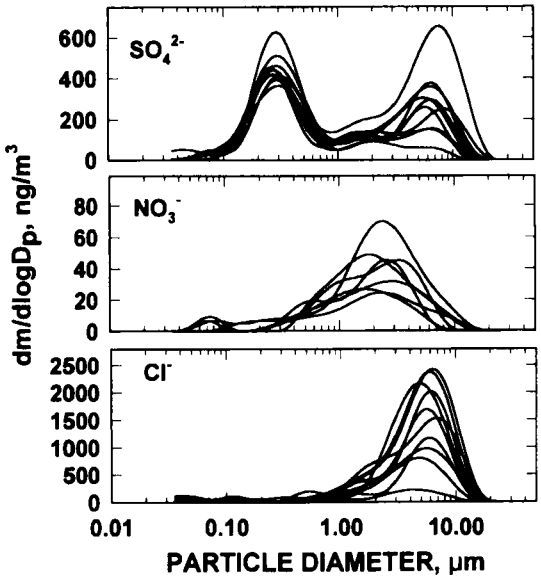

FIGURE 3 Size distributions of anions. Particle diameter is aerodynamic

Over the fine-particle size range (aerodynamic diameter less than 1 μm), complete data sets were obtained for sulphate and ammonium only. However, ammonium data of runs 9 and 10 were not used because they were analyzed after the field campaign in a chemical laboratory, and could have been contaminated by ammonia during the storage. For chloride, nitrate, sodium and magnesium, size distributions were obtained from a total of 5 to 8 runs. Calcium and potassium concentrations, in this case. were also too low to distinguish them from the relative high blank values of the extract solution.

Excluding sulphate, the observed ions were associated primarily with either fine or coarse particles. Overall, the measured mass size distributions displayed four separate modes. The Aitken mode, representing particles smaller than about 0.1 μm in diameter, consisted probably of aerosols formed in the Antarctic marine atmosphere. The accumulation mode with a particle diameter between 0. and 1 μm. had particles grown from the Aitken-mode by cloud processing,

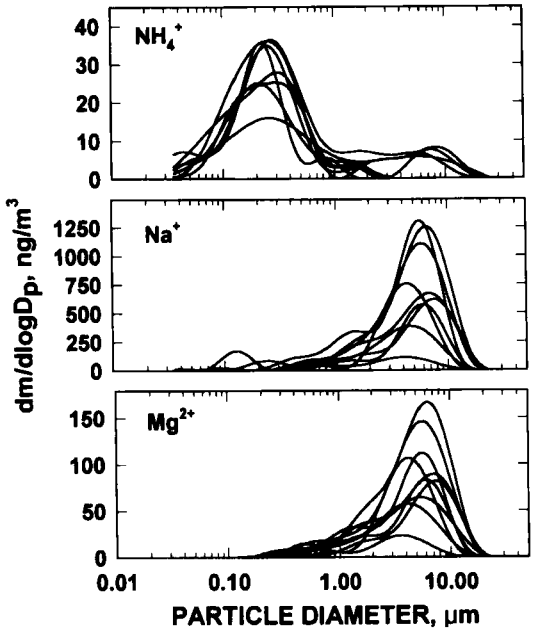

FIGURE 4 Size distributions of cations. Particle diameter is aerodynamic

sea-salt particles emitted from the ocean, and possibly some long-range-transported particles from remote continental sources. The two overlapping coarse-particle modes were primarily sea-salt particles.

For each ion and run, the log-normal modal parameters were calculated. The statistics of these calculations is summarized in Table IV. The averaged data were used further to compare the mass concentration ratios of ions in the atmosphere to the respective ratios in the sea water. The results of this comparison are shown in Table V. For the upper supermicron mode (mode 4), the ratios of sulphate to sodium. sodium to chloride and magnesium to sodium, are very close to those in the sea water. This mode consists most likely of relatively fresh sea-salt particles. The lower supermicron mode (mode 3) is enriched in sulphate, while other concentration ratios are again close to those in the sea water. Mode 3 evidently represents sea-salt particles experienced some uptake of sulphate during their residence in the atmosphere. The concentrations of sea salt particles (Table IV) and the modal nature is in agreement with the observations of Wyputta [20]. In their study at the Georg-von-Neumayer station in Antarctica it was found that sea salt particles consist of particles produced by wind-induced bubble bursting at the ocean surface and of primary aerosols of local origin for coastal stations.

TABLE IV Average log-normal parameters of size distributions. Standard deviation for each parameter is shown in parenthesis. D_p is the aerodynamic mass mean diameter, σ_g is the geometric standard deviation and N the number of distributions. Concentrations are in units ng/m^3

Ion	*Mode 1*				*Mode 2*				*Mode 3*				*Mode 4*			
	D_p,μm	σ_g	*Conc.*	*N*	D_p,μm	σ_g	*Conc.*	*N*	D_p,μm	σ_g	*Conc.*	*N*	D_p,μm	σ_g	*Conc.*	*N*
SO_4^{2-}	0.069	1.29	7.89	9	0.285	1.63	238.8	10	1.83	1.72	74.0	10	6.56	1.55	138	10
	(0.011)	(0.09)	(5.05)		(0.016)	(0.07)	(39.7)		(0.31)	(0.13)	(22.3)		(0.80)	(0.06)	(91)	
NH_4^+	0.087	1.80	4.40	7	0.270	1.83	18. 1	8	1.96	1.58	2.29	8	6.69	1.57	3.38	2
	(0.036)	(0.31)	(2.77)		(0.049)	(0.26)	(4.64)		(1.40)	(0.44)	(1.86)		(1.13)	(0.05)	(0.21)	
NO_3^-	0.100	1.39	2.50	4	0.536	1.65	6.07	7	2.18	1.90	26.3	7	6.15	1.56	9.66	4
	(0.050)	(0.12)	(0.43)		(0.174)	(0.22)	(3.17)		(0.66)	(0.18)	(10.6)		(2.29)	(0.12)	(10.07)	
Cl^-	0.080	1.38	7.84 (	1	0.423	1.44	31.4	5	1.71	1.80	230	9	5.71	1.63	774	10
	(–)	(–)	-)		(0.171)	(0.09)	(22.6)		(0.54)	(0.27)	(150)		(0.84)	(0.08)	(372)	
Na^+	-	-	-	-	0.506	1.43	30.6	8	1.67	1.84	152	8	5.75	1.67	476	10
					(0.155)	(0.13)	(11.3)		(0.44)	(0.22)	(72)		(1.10)	(0.09)	(218)	
Mg^{2+}	-	-	-	-	0.536	1.50	6.42	6	1.71	1.86	18.6	7	5.58	1.68	51. 1	10
					(0.144)	(0.19)	(4.58)		(0.45)	(0.20)	(9.7)		(1.31)	(0.11)	(19.0)	

TABLE V Ratios of modal mass concentrations compared to ratios in sea water

Ratio	*Mode 2*	*Mode 3*	*Mode 4*	*Sea water**
SO_4^{2-}/Na^+	7.80	0.49	0.29	0.25
Na^+/Cl^-	0.97	0.66	0.61	0.55
Mg^{2+}/Na^+	0.21	0.12	0.1 1	0.13

* According to CRC Handbook of Chemistry and Physics (1989)

The dominating ion in the accumulation mode (mode 2) is sulphate. The ratio of Na^+ to Cl^- in this mode is larger than that in the sea water, which can be explained by the reaction of sulphuric and nitric acids with NaCl and $MgCl_2$ in the sea-salt particles, and subsequent evaporation of HCl from these particles [21]. As shown later in the text, the accumulation mode plausibly is an external mixture of relatively neutral sea-salt particles and more acidic ammonium-sulphate/hydrated sulphuric acid particles.

Table VI shows the average modal concentrations of each ion, expressed in units neq/m^3. The anion to cation ratios of modes 3 and 4 are 1.02 and 0.988, respectively. The apparent balance of ion charges for supermicrometer particles suggests them to be approximately neutral. The respective ratio in the accumulation mode (mode 2) is 2.49, which can be ascribed to the presence of H^+ not measured in this study. If we assume an external mixture of sea-salt and ammonium-sulphate particles in the accumulation mode, the anion to cation ratio of the latter ones is as high as 4.81, making these particles extremely acidic. A consequence of this is the relatively strong acidity of precipitation observed in Antarctica by surface snow and ice core measurements [22].

TABLE VI Average modal concentrations in neq/m^3. Also shown are the calculated non-sea salt SO_4^{2-} concentration, and total concentrations of anions and cations.

	Total SO_4^{2-}	*nss-*SO_4^{2-}*	NH_4^+	NO_3^-	Cl^-	Na^+	Mg^{2+}	*Anions*	*Cations*
Mode 1	0.16	-**	0.24	0.04	0.55	-	-	0.75	0.24
Mode 2	4.97	4.81	1.00	0.10	0.89	0.86	0.53	5.96	2.39
Mode 3	1.54	0.75	0.13	0.42	6.49	6.61	1.53	8.45	8.27
Mode 4	2.87	0.40	0.19	0.16	21.8	20.7	4.20	24.8	25. 1

* Calculated using a mass ratio of 0.25 for SO_42-/Na^+ in sea water
** Not calculated due to lack of Na^+ data

Sulphate

Atmospheric sulphate originates almost entirely from SO_2 emitted directly by many anthropogenic sources, and from DMS released by oceans. The lifetimes of particulate sulphate and its precursors commonly are no longer than a few days in the atmosphere, which makes the flux of long-range-transported anthropogenic sulphate to Antarctica quite small [4]. The dominant source of sulphate measured in this study thus is expected to be DMS emitted by the high-latitude Antarctic oceans.

The conversion of SO_2 to particulate sulphate occurs via multiple pathways. In a global scale, from 50 to 90% of the sulphate is estimated to be formed by the oxidation of dissolved SO_2 in cloud droplets [23]. This mechanism generates sulphate primarily to the accumulation mode. During sunlit hours, gas-phase oxidation of SO_2 produces sulphuric acid, most of which condenses on preexisting submicrometer particles. If ambient conditions are favourable, a portion of gaseous sulfuric acid nucleates with water vapour to form new, nanometer-size particles. In the marine boundary layer, an important mechanism producing particulate sulphate has been speculated to be the oxidation of SO_2 by ozone in the water absorbed by sea-salt particles [24]. This oxidation process is very rapid, with most of the non-sea-salt sulphate formed during the first ten minutes as the emitted sea-salt particles still are alkaline.

The measured sulphate mass size distributions had typically four modes (Figure 3). The time series of sulphate concentrations in each of these modes are shown in Figure 5. On average, more than 70% of the non-sea-salt sulphate can be found in the accumulation mode (0.1–1.0 μm). The concentration of the accumulation-mode sulphate is very stable over the sampling period, implying that its sources are relatively uniformly distributed around the measurement site.

The existence of an Aitken mode in the size range 0.05–0.09 μm is indicative of new particle production in the Antarctic atmosphere. This is consistent with the observations of Gras [14] and Ito [4], according to which high Aitken-particle number concentration are a semi-permanent feature of the Antarctic summer atmosphere.

The accumulation mode had a mass median diameter between 0.25–0.30 μm (Figure 6). The variation of the modal size between different runs reflects changes in the ambient relative humidity (Table VII), as well as differences in the amount of sulphate collected by these particles via cloud processing. For comparison, Kerminen et al. [18] observed modal mass median diameters of 0.31 and 0.28 μm for sulphate and MSA, respectively, in clean summer air masses arriving at the Finnish Arctic from the high Arctic ocean.

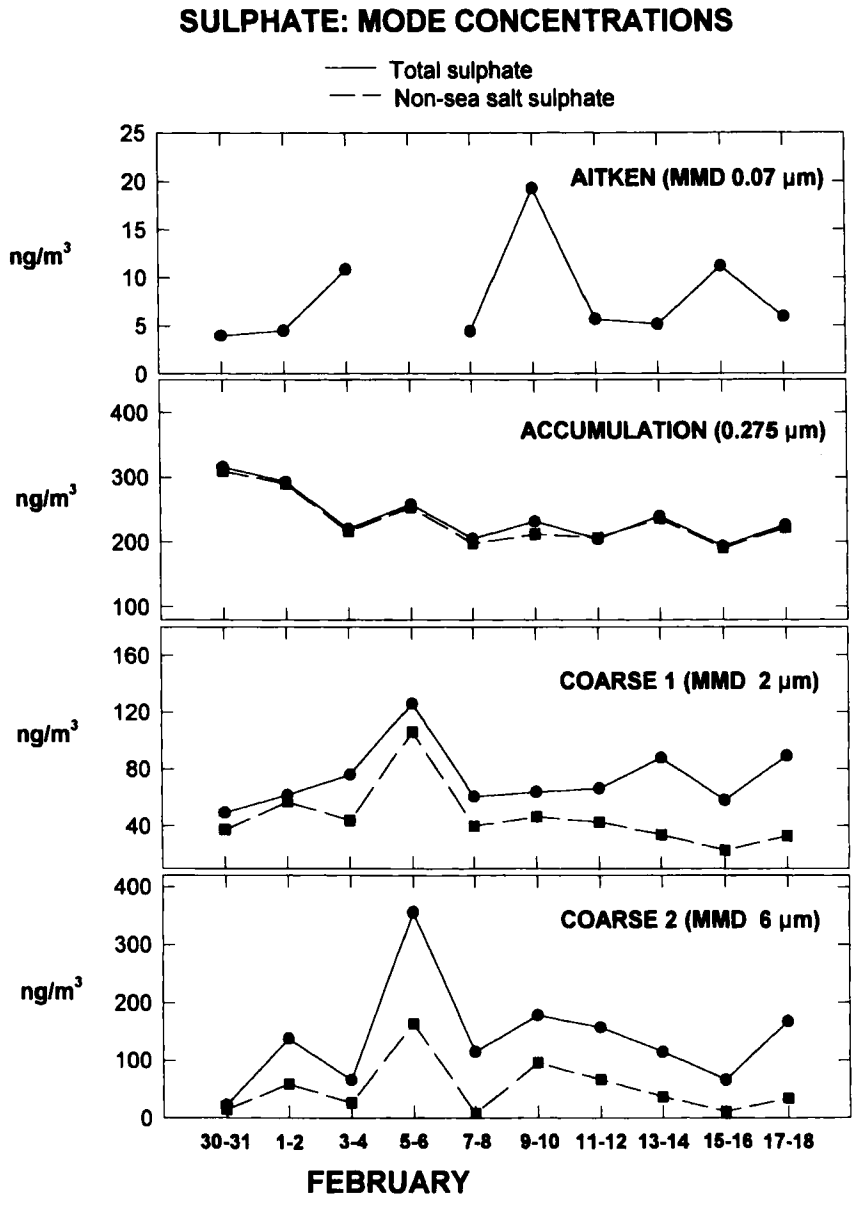

FIGURE 5 Modal concentrations for total and non-sea-salt sulphate

TABLE VII Relative humidity data for impactor runs

Run #	*Date*	*Relative humidity, %*	
		Average (Standard deviation)	*Range*
1	Jan 30–31	36.0 (12.4)	21.9 – 60.7
2	Feb 1–2	38.2 (16.1)	20.1 – 62.0
3	3–4	38.5 (10.0)	21.6 – 53.4
4	5–6	35.8 (12.9)	21.6 – 58.6
5	7–8	49.0 (19.4)	20.0 – 77.5
6	9–10	41.6 (14.8)	20.0 – 66.2
7	11–12	51.5 (20.7)	27.7 – 75.8
8	13–14	54.9 (17.1)	32.4- 81.5
9	15–16	43.4 (5.9)	34.8 – 52.8
10	17–18	37.7 (3.5)	32.9 – 44.9

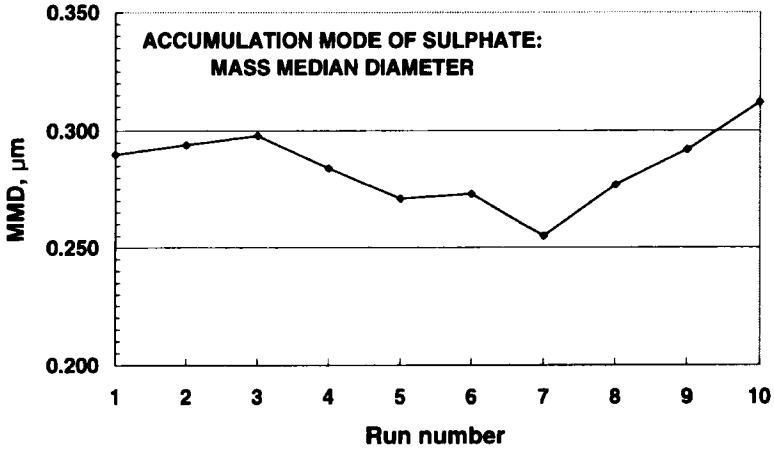

FIGURE 6 Aerodynamic mass median diameter of accumulation mode sulphate. The dates corresponding to each run are given in Fig. 5 and in Table VII

The non-sea-salt sulphate found in the coarse-particle range followed closely the concentrations of typical sea-salt ions Na^+ and Cl^- (Figure 5). The enrichment of sulphate with respect to sea water was greater for the lower supermicron

mode, as expected due to longer atmospheric residence times of smaller coarse particles. Potential mechanisms for the formation of excess supermicron sulphate are i) the condensation of gaseous sulphuric acid into the sea-salt particles, ii) the reaction of gaseous SO_2 on the surface of these particles, and iii) the oxidation of dissolved SO_2 by ozone in the water absorbed by the particles. The first two processes are expected to distribute sulphate close to the surface-area size distribution of the sea-salt; ozone-oxidation will distribute it closer to the respective mass size distribution [25].

The mass and surface-area median diameters of sodium, and the mass median diameter of sulphate, for both the supermicron modes and for each run, are plotted in Figure 7. The lower-mode sulphate seems to be distributed close to the surface-area distribution of Na in run 6, suggesting domination of the processes (i) and (ii) in accumulating sulphate to the sea-salt particles in this mode. The other runs show either that process (iii) dominates or they are combinations of all processes. The mass median diameter of the upper-mode sulphate is of the same order or even greater than that of sodium, supporting the domination of the process (iii). The large median size of this upper sulphate mode may partially be explained by the uptake of sulphate by large soil particles derived from the Antarctic continent.

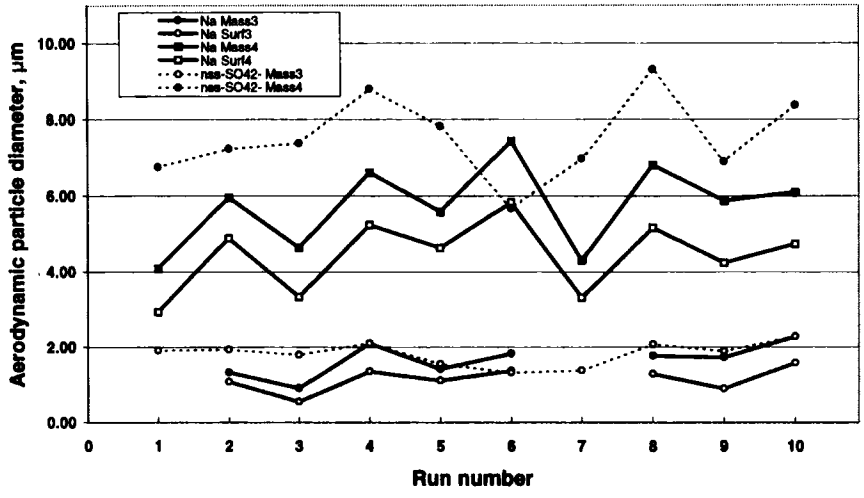

FIGURE 7 Non-sea-salt sulphate mass median diameters compared with the median diameters of sodium mass and surface area distributions. In legend Mass stands for mass distribution and Surf for surface area distribution, the following number 3 or 4 refers to lower and upper coarse particle modes, respectively

Nitrate

Nitrate originates from the transport of gaseous nitric acid to the particulate phase, and from the reaction of NO_2, NO_3 or N_2O_5 with the particles [26]. Reaction of nitrogen species with sea-salt particles is an important sink for atmospheric nitrogen and, together with the reaction between sulphur gases and sea-salt particles, a dominant source of atmospheric HCl in remote locations [27].

In this study, a major fraction of the nitrate was found in the coarse-particle size range, where it typically had a mass median diameter of around 3–4 μm. As shown by Figures 3 and 4, supermicron nitrate was shifted towards smaller sizes than $Na^+$and Cl. This kind of distribution is expected in light of the formation of nitrate on sea-salt particles. In fact, when the Na mass median diameter is converted to the respective surface-area diameter, it is in some cases close to the mass median diameter of nitrate (Figure 8). A portion of the supermicron nitrate may originate from the reaction of nitric acid with soil-derived particles, as has frequently been observed at various coastal and continental sites [28].

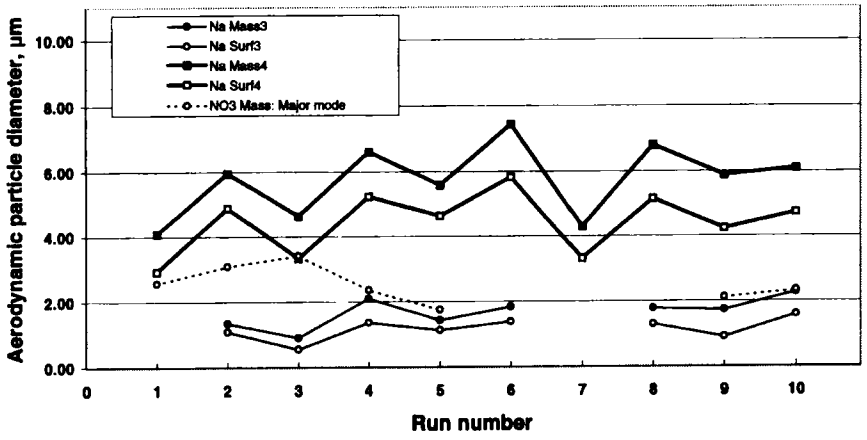

FIGURE 8 Nitrate mass median diameters compared with the median diameters of sodium mass and surface area distributions. In legend Mass stands for mass distribution and Surf for surface area distribution, the following number 3 and 4 refer to lower and upper coarse particle modes, respectively. Of two coarse particle nitrate modes the major mode is used in the comparison

An interesting feature is the presence of nitrate in the accumulation mode. If these particles were internally mixed, they should contain practically no nitrate nor chloride because of their high sulphate to cation ratio. The problem can be avoided by assuming the accumulation mode to be an external mixture of sea-salt and ammonium-sulphate particles. This view is supported by the mass median

diameters of individual ions in the accumulation mode (Table IV): SO_4^{2-}. and NH_4^+ clearly form their own group; Na^+, Cl^-, Mg^{2+} and NO_3^- their own. The measured nitrate concentrations are sufficiently high to be responsible for most of the chloride depletion from the sea-salt particles in the accumulation mode. From Table VI we can estimate further that, on average, sea-salt accounts for about 20% (in neq/m^3) of the measured inorganic ions in the accumulation mode.

Ammonium

Ammonium was distributed over the whole particle size range, with on average 80% found in submicrometer particles. In Figure 9 ammonium mass size distributions (in neq/m^3) are compared with those of sulphate. The concentrations of accumulation-mode ammonium show some variability between the different runs, but behave in general quite similarly to sulphate. The variation of Aitken-mode ammonium concentration is much greater.

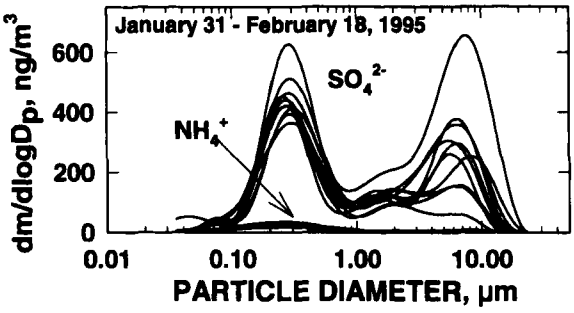

FIGURE 9 Sulphate and ammonium size distributions in neq/m^3

Since particulate ammonium is formed via condensational gas-to-particle conversion only, the Aitken mode should be more identifiable from ammonium than from sulphate mass size distributions. Figures 3 and 4 show that this indeed might be the case, although some precautions are due to a risk of contamination of acid samples by ammonia during handling. The large variability of Aitken-mode ammonia reflects the greater variability of Aitken-mode particle counts in measured air masses compared with accumulation-mode particles. For run 1 the Aitken mode concentrations of SO_4^{2-}, NH_4^+, NO_3^- and Cl^- are 0.082, 0.168, 0.045 and 0.221 neq/m^3, respectively. The relatively high concentrations of Cl^- in the Aitken mode suggests that part of the ammonium may be there as ammonium chloride. Because only one complete set of major ions in Aitken

mode was available, more studies are needed to confirm if this is a general feature in Antarctic boundary layer atmosphere.

CONCLUSIONS

Aerosol particles and their gaseous precursors were studied at a coastal Antarctic site during the austral summer January-February, 1995. A dominant fraction of the observed particles and gases were related to maritime emissions and the subsequent reactions in the atmosphere. The anthropogenic contribution, although not quantified, was probably rather small. The accumulation mode consisted obviously of an external mixture of sea-salt related and ammonium-sulphate/hydrated sulphuric acid particles. The latter population was estimated to have an average anion to cation equivalent ratio of 4.86, indicating that these particles were extremely acidic. Coarse sea-salt particles play a central role in the Antarctic tropospheric chemistry. The deposition flux of sulphur and nitrogen species is significantly enhanced due to the reaction of SO_2 and HNO_3 with sea-salt particles. Both pathways release in addition HCl gas into the atmosphere. HCl, which concentrations were not possible to draw from denuder data of this study, is probably an important agent in inorganic and organic atmospheric chemistry in Antarctica. Concentrations of SO_2 measured in this study were close to those observed before during summer in Antarctic boundary layer atmosphere. Also NH_3concentrations measured in the present study are in agreement with previous studies and suggest that ammonia is an important neutralizing agent in Antarctic atmosphere.

Acknowledgements

R. E. H. and V.-M.K. are grateful to the Maj and Tor Foundation and to the Academy of Finland for the financial support of this study. This work was done when R.E.H. was in Italy within the Human Capital and Mobility fellowship (EC contract Nr ERBCHBICT941759). The authors will thank Dr. Willy Maenhaut from the University of Gent for providing the mode fitting software.

References

[1] J. L. Gras. *Atmos. Environ.* **17**, 815–818 (1983).
[2] G. E. Shaw. *Atmos. Environ.* **14**, 911–921 (1980).
[3] D. L. Savoie, J. M. Prospero, R. J. Larsen and E. S. Saltzman. *J. Atmos. Chem.* **14**, 181–204 (1992).
[4] T. Ito. *Tellus* **45B**, 145–159 (1993).
[5] J. E. Penner, R. J. Charlson, J. M. Hales, N. S. Laulainen, R. Leifer, T. Novakov, J. Ogren, L. F. Radke, S. E. Schwartz, and L. Travis. *Bull. Amer. Meteor. Soc.* **75**, 375–400 (1994).
[6] J. F. B. Mitchell, T. C. Johns, J. M. Gregory and S. F. B. Tett. *Nature* **376**, 501–504 (1995).

[7] C. Pilinis, S. N. Pandis and J. H. Seinfeld. *J. Geophys. Res.* **100**, 18,739–18,754 (1995).
[8] J.-F. Müller. *J. Geophys. Res.* **97**, 3787–3804 (1992).
[9] M. Pham, J.-F. Müller, G. P. Brasseur, C. Granier and G. Megie. *J. Geophys. Res.* **100**, 26,061–26,092 (1995).
[10] M. O. Andreae, W. Elbert and S. J. de Mora. *J. Geophys. Res.* **100**, 11,335 – 11,356 (1995).
[11] I. Allegrini, M. Montagnoli, R. Sparapani. *Intern. J. Environ. Anal. Chem.* **55**, 267–283 (1994).
[12] A. Berner and C. Lürzer. *J. Phys. Chem.* **84**, 2079–2083 (1980).
[13] B. Y. H. Liu and D. Y. H. Pui. *Atmos. Environ.* **15**, 589–600 (1981).
[14] J. L. Gras. *Atmos. Environ.* **27A**, 1427–1434 (1993).
[15] J. K. Wolfenbarger and J. H. Seinfeld. *SIAM J. Sci. Stat. Comput.* **12**, 342–361 (1990).
[16] H. C. Wang and W. John. *Aerosol Sci. Technol.* **8**, 157–172 (1988).
[17] R. E. Hillamo and E. I. Kauppinen. *Aerosol Sci. Technol.* **14**, 33–47 (1991).
[18] V.-M. Kerminen, M. Mäkinen, R. E. Hillamo and A. Virkkula. *Tellus*, in press (1997).
[19] W. Winklmayr, H.-C. Wang and W. John. *Aerosol Sci. Technol.* **13**, 322–331 (1990).
[20] U. Wyputta. *Tellus* **49B**, 93–111 (1997).
[21] M. Posfai, J. R. Anderson, P. R. Buseck and H. Sievering. *J. Geophys. Res.* **100**, 23063–23074 (1995).
[22] M. Legrand. In: R. J. Delmas (ed.) *Ice Core Studies of Global Biogeochemical Cycles.* NATO ASI Series, Vol. I 30, Springer-Verlag Berlin Heidelberg, pp 91–119 (1995)
[23] J. Langner and H. Rodhe. *J. Atmos. Chem.* **13**, 225–263 (1991).
[24] H. Sievering, E. Gorman, T. Ley, A. Pszenny, M. Springer-Young, J. Boatman, Y. Kim, C. Nagamoto and D. Wellman. *J. Geophys. Res.* **100**, 23075–23081 (1995).
[25] V.-M. Kerminen and A. S. Wexler. *Atmos. Environ.* **29**, 3263–3275 (1995).
[26] Y. Mamane and J. Gottlieb. *Atmos. Environ.* **26A**, 1763–1769 (1992).
[27] A. Eldering, P. A. Solomon, L. G. Salmon, T. Fall and G. E. Cass. *Atmos. Environ.* **25A**, 2091–2102 (1991).
[28] T. A. Pakkanen, V.-M. Kerminen, R. E. Hillamo, M. Mäkinen, T. Mäkelä and A. Virkkula. *J. Atmos. Chem.* **24**, 189–205 (1996).